ResearchGate

See discussions, stats, and author profiles for this publication at: https://www.researchgate.net/publication/380912120

A new approach to designing a multiband antenna using photonic crystals and load graphene for terahertz application

Article *in* Results in Engineering · June 2024

DOI: 10.1016/j.rineng.2024.102327

CITATIONS
0

READS
122

5 authors, including:

Amraoui Youssef
Sidi Mohamed Ben Abdellah University
5 PUBLICATIONS **8** CITATIONS
SEE PROFILE

Imane Halkhams
Sidi Mohamed Ben Abdellah University
36 PUBLICATIONS **108** CITATIONS
SEE PROFILE

Rachid El Alami
Sidi Mohamed Ben Abdellah University
43 PUBLICATIONS **147** CITATIONS
SEE PROFILE

mohammed Ouazzani jamil
Université Privée de Fès
99 PUBLICATIONS **454** CITATIONS
SEE PROFILE

All content following this page was uploaded by Amraoui Youssef on 29 May 2024.

The user has requested enhancement of the downloaded file.

Results in Engineering 22 (2024) 102327

Contents lists available at ScienceDirect

Results in Engineering

journal homepage: www.sciencedirect.com/journal/results-in-engineering

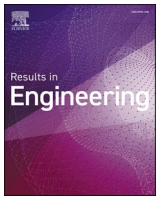

A new approach to designing a multiband antenna using photonic crystals and load graphene for terahertz application

Amraoui youssef [a,*], Imane Halkhams [b], Rachid El Alami [a], Mohammed Ouazzani Jamil [b], Hassan Qjidaa [a]

[a] LISAC Laboratory, Sidi Mohamed Ben Abdellah University, Fez, Morocco
[b] SIEDD Laboratory, Private University of Fez, UPF, Fez, Morocco

ARTICLE INFO

Keywords:
Terahertz antenna
Photonic crystal
Graphene
Patch antenna
PBG
Multiband

ABSTRACT

The primary concern addressed in this article is the inherent difficulty in creating antennas capable of effectively operating across a range of frequency bands within the terahertz (THz) spectrum. Conventional antenna designs often fall short in terms of delivering the required bandwidth and power for such applications. To mitigate this problem, we present a technique that uses photonic crystals integrated into the antenna design to generate photonic band gaps (PBG) with the graphene loaded in the THz band. So, the purpose was to find the optimal multiband antenna that can function across 1.13 and 0.65 THz. Simulations were conducted for rectangular patch antennas using different types of substrates, which included homogeneous, periodic, and aperiodic photonic crystal substrates, and by using a graphene load, simulations were carried out. Multiple sets of air holes (rectangular and cylindrical) were punched into the polyimide substrate of each modified photonic crystal substrate, and the load graphene was placed in the patch. The anticipated multiband antenna design has successfully achieved impressive performance metrics, including a minimal reflection coefficient of −36.8 dB and −41.812 dB, a substantial bandwidth of 25 GHz, and 110 GHz at 0.65 THz and 1.13 THz, respectively. Additionally, the design boasts a gain of 6.44 dBi, 9.45 dBi, and a remarkable radiation efficiency of 75.12 % and 80.03 %, respectively, with a VSWR <2 at the resonating frequencies. The distinctive attributes of PBG, combined with the multiband capabilities of the antenna, position it as a highly promising option for terahertz imaging systems like those used for detecting concealed objects in settings such as airports. Furthermore, its potential extends to biomedical imaging, where it could be utilized to identify tissue irregularities with improved clarity and contrast.

1. Introduction

The utilization of the terahertz (THz) spectrum, covering the range of 10^2 GHz−10 THz [1], is widespread in modern communication systems due to its numerous advantages. Firstly, terahertz waves are well suited for non-contact detection since they have remarkable penetrating properties for opaque, non-polar, dry materials, including porcelain, semiconductors, paper, cloth, polymers, and other non-metallic substances [2]. Secondly, THz waves are non-ionizing, characterized by low photon energy, and harmless to biomolecules and materials. This quality makes them an ideal choice for non-destructive testing [3]. Thirdly, their higher frequencies compared to microwaves enable applications in various scenarios with high-speed communication capabilities and ultrawideband [4], including terahertz radars and antennas [5]. Furthermore, terahertz waves, renowned for their exceptional imaging resolution, have been utilized in medical imaging since 1995 and have been applied in non-contact, non-invasive, imaging techniques and non-ionizing biosensing [6]. Specifically, this frequency range holds significant relevance for a variety of intriguing applications in astronomy, biomedical, and communication [7–9]. The development of THz antennas and devices is a new trend in wireless communication systems. The existing challenge in THz antennas lies in achieving a desirable frequency response while maintaining high gain and meeting other far-field performance criteria [10]. Achieving high gain represents a fundamental necessity for THz antennas, given that atmospheric path loss is significantly elevated at these higher frequencies.

The creation of multiband antennas that can operate well over a variety of frequency ranges is a difficult task [11], especially in the

* Corresponding author.
E-mail address: youssef.amraoui2@usmba.ac.ma (A. youssef).

https://doi.org/10.1016/j.rineng.2024.102327
Received 26 March 2024; Received in revised form 23 May 2024; Accepted 26 May 2024
Available online 27 May 2024
2590-1230/© 2024 The Authors. Published by Elsevier B.V. This is an open access article under the CC BY-NC-ND license (http://creativecommons.org/licenses/by-nc-nd/4.0/).

terahertz (THz) band, where atmospheric circumstances interfere with signal propagation. To overcome this obstacle and unlock the potential of THz communication, enhancing antenna performance is a critical objective. Incorporating photonic crystals into the antenna substrate is a promising approach. Since their discovery. Yablonovitch and John introduced the concept of photonic crystals in 1987 [12], which may manifest in one-dimensional (1D), two-dimensional (2D), or three-dimensional (3D) configurations. Photonic crystals have garnered significant and swift attention in recent times, resulting in their widespread application for creating exceptionally efficient electromagnetic and optical devices across different fields and applications. This emerging multidisciplinary field holds the potential to enable a large number of applications. One of the potential forthcoming applications entails the development of a microstrip antenna that uses a structural arrangement of photonic crystals as its substrate, to suppress undesired surface waves excited within the substrate. Such an approach would not only enhance antenna efficiency but also maintain reduced side lobe levels by mitigating surface wave diffraction at the antenna substrate's edges [13]. These surface waves tend to be more pronounced when thick substrates are utilized. PBG structures are artificial periodic (or aperiodic) configurations consisting of hollow air cylinders with various shapes, such as elliptical, triangular, hexagonal, and circular, which can be embedded within the dielectric substrate material. In the quest for a high-performance THz microstrip antenna, the adoption of a photonic band gap (PBG) substrate, as discussed in Ref. [14], emerges as a compelling approach. This entails integrating various materials such as metallic, dielectric, and ferromagnetic elements into the substrate cavity. The PBG substrate boasts a distinctive attribute known as the frequency band gap, effectively constraining the propagation of electromagnetic waves within a specified frequency range by periodically altering the dielectric constant. This manipulation of the frequency band gap holds promise for suppressing surface wave loss, reducing return loss, and amplifying antenna gain, as outlined in Ref. [15]. Research conducted previously highlights the common application of the air-hole PBG substrate in developing single-frequency THz microstrip antennas, aiming to reduce return loss and enhance gain [16–20]. The air-hole PBG antenna has the capability for multi-band operation but does not lead to significant gain improvements.

Graphene's primary appeal lies in its potential as a strong contender for the advancement of THz antenna systems [21,22]. This is primarily due to its minimal skin effect and the ability to adjust its properties through chemical or electrostatic gating. These unique characteristics have enabled researchers to create a range of graphene-based antennas with remarkable capabilities at terahertz frequencies. Ensuring the structural integrity of graphene during its integration into the antenna structure is crucial due to its sensitivity to environmental conditions and susceptibility to degradation. To tackle this challenge, employing chemical vapour deposition (CVD) for synthesizing graphene directly onto the substrate proves effective in preserving its quality. Moreover, implementing rigorous handling and transfer procedures within cleanroom environments can mitigate the risk of contamination and defects, thereby safeguarding the antenna's optimal performance. In light of this, the integration of photonic crystals into the construction of a graphene-based terahertz antenna is poised to enhance its radiation performance. At a frequency of 0.65 THz, a terahertz antenna featuring graphene and a photonic crystal structure has been proposed [23]. Utilizing graphene, a microstrip antenna design has been created on a silicon-air photonic band gap substrate [24]. An extensively broad and high-gain patch antenna for terahertz applications, employing graphene, has been documented [25]. Additionally, various methods have been employed to create dual-band antennas based on graphene. In Ref. [26], a reconfigurable dual-band THz patch antenna is suggested, utilizing a backing cavity based on a graphene stack. A dual-band antenna with optical transparency, employing Indium Tin Oxide (ITO), has been created for THz communication [27]. Graphene dual-band antennas have also been achieved by modifying the substrate's thickness, as outlined in Ref. [28]. In this topic, numerous antenna configurations have been documented, along with simulation investigations, for THz applications. The authors in Ref. [29] showcase the creation of a patch antenna with a trapezoidal shape achieved by incorporating photonic crystals into the substrate layer to generate photonic band gaps. The antenna has been developed for utilization in the frequency range spanning from 0.88 to 1.62 THz, specifically tailored for high-speed applications. In Ref. [30], a compact terahertz (THz) rectangular microstrip antenna with a wide bandwidth of 26.4 GHz and diminutive dimensions measuring $180 \times 210 \times 10\ \mu m^3$ has been introduced. This antenna design incorporates a PBG substrate and a defected ground structure, which have been thoroughly examined. The final antenna configuration resonates at a central frequency of 0.703 THz, boasting an impressive return loss of −50.94 dB. Additionally, the recommended antenna exhibits a gain of 5.075 dBi and a directivity of 6.833 dBi. Its voltage standing wave ratio (VSWR) is exceptionally low at 1.006. In Ref. [31], a MIMO antenna structure with a fractal design is situated on a SiO2 substrate that incorporates a PBG. This MIMO antenna configuration, as designed, attains an outstanding impedance bandwidth of 1590 GHz. Additionally, the recommended antenna features a gain of 4.6 dBi and a radiation efficiency of 74 % at 1.89 THz. In Ref. [32], the antenna design incorporates a graphene radiator and employs a Gallium Arsenide substrate, enabling operation at frequencies of 2.1, 1.9, and 1.4 THz. Various photonic crystal substrates with hexagonal, triangular, cylindrical, and square shapes are examined. Simulation outcomes reveal that hexagonal-shaped photonic crystals yield impressive performance metrics, including a broad emission spectrum bandwidth spanning 220 GHz, an efficiency of 98 %, an axial ratio of 29 dB, and a directivity of 15 dBi. In Ref. [33], a groundbreaking antenna array design concept is introduced. This design aims to enhance radiation characteristics by utilizing graphene-based materials and employing different substrates, including a homogeneous substrate, a photonic bandgap crystal substrate, and a superstrated dielectric grating. Remarkable performance metrics are achieved, including a directivity of 15.5 dBi at 0.8883 THz, a significant gain of 14.69 dB, and a minimum reflection coefficient of −57.052 dB. So, the fundamental goal of this research is to innovate and develop a new terahertz antenna design. This antenna should exhibit two crucial qualities: an exceptionally high gain for improved signal performance and an extraordinarily wide bandwidth to cover a wide range of frequencies. Importantly, this must be achieved while keeping the antenna's size compact, which is essential for its practical use in terahertz applications. This article presents an innovative methodology for the development and design of multiband patch antennas specifically tailored for THz applications by introducing a graphene load into the radiating element. The key innovation lies in the incorporation of photonic crystals into the antenna's structure to generate photonic band gaps, enabling precise control over electromagnetic wave propagation and consequently enhancing the antenna's performance across the 0.3 to 1.25 THz frequency range.

Utilizing photonic crystals enables the creation of PBG, which selectively filters frequencies to enhance the antenna's effectiveness across various THz bands. This approach facilitates achieving the desired frequency response and improving the overall antenna performance. Additionally, the integration of graphene into the antenna patch represents a significant progression, owing to graphene's exceptional electrical properties, which afford greater control over resonant frequencies, increased conductivity, and enhanced antenna gain and efficiency.

Compared to GHz-ranged microstrip patch antennas, our THz antenna provides several key advantages; the higher frequencies of the THz spectrum enable much higher resolution imaging and spectroscopy, which is essential for detailed analysis of molecular and biological tissues. Additionally, the THz spectrum offers significantly broader bandwidths, allowing for high-speed data communication and precise spectroscopic analysis. Furthermore, THz waves have greater sensitivity for detecting materials and biological tissues, improving the

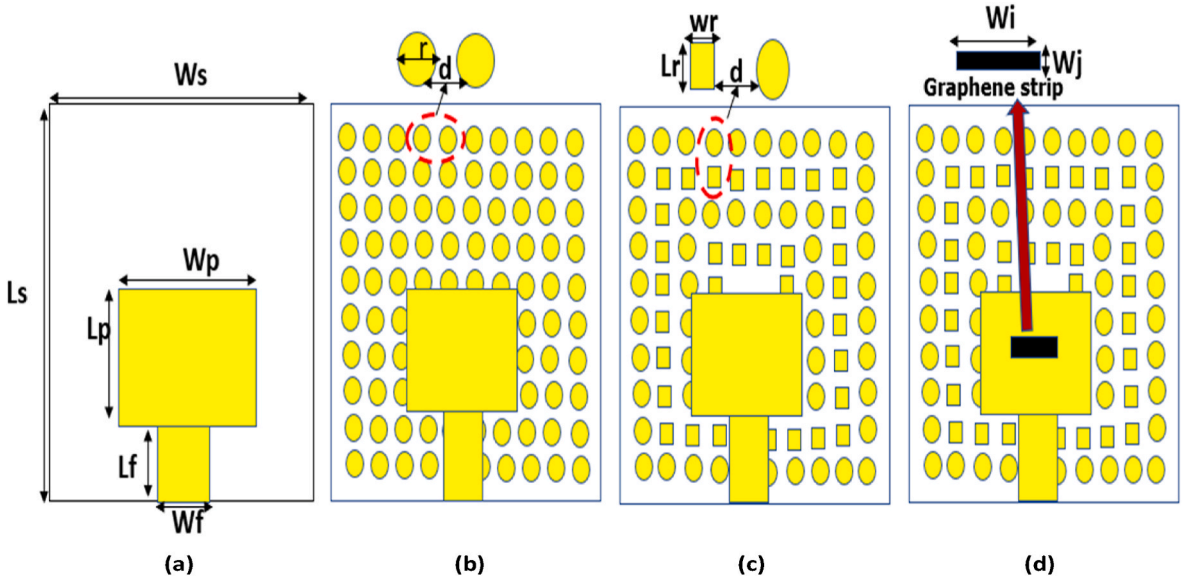

Fig. 1. Different variants of the recommended THz design (a) Ant I (b) Ant II (c) Ant III, and (d) Ant VI.

effectiveness of applications such as chemical spectroscopy, which enables precise molecular detection, and advanced medical imaging, which provides high-resolution tissue imaging. In this document, we provide a concise overview of the novelty and key performance parameters as follows.

- The suggested antenna design offers multi-band operation with significantly low return loss. This characteristic effectively minimizes interference among the individual antenna elements, contributing to improved overall performance.
- This antenna design achieves impressive high gain values of 6.44 dBi and 9.45dBi during its multiple frequency bands.
- In the frequency spectrum spanning from 0.3 to 1.25 THz, this antenna structure delivers an ultra-wideband operation (25 GHz, 110 GHz at resonating frequencies).
- The performance of the recommended antenna is evaluated against previously published antenna structures. These comparisons reveal that the suggested antenna is not only compact but also provides multiband operation and achieves high radiation gain values.

This document is arranged in the following manner: Section 2 outlines the design of the recommended antenna utilizing photonic crystal. Section 3 encompasses the simulation and evaluation of the recommended antenna. Finally, the paper concludes in Section 4.

2. Evolution of the suggested multiband antenna

The design specifics of the recommended multiband antennas, which are suited for utilization in the THz frequency band, are covered in this section. In this context, polyimide served as the substrate material, with defined a loss tangent of 25. 10^{-2} and a dielectric constant of 3.5 as shown in Fig. 1. The patch is made by using copper with LP and Wp positioned on the upper side of the substrate material. Additionally, the ground plane is composed of copper and has a thickness of 0.1 μm. The overall dimensions of the antenna measured 700 × 660 × 192 μm^3. A substrate utilizing PBG principles has been etched onto the polyimide substrate, incorporating graphene to augment the performance of the antenna design. The PBG structure has been crafted by introducing regularly spaced air gap cylinders onto the substrate. Here, graphene's electrical properties are specified with chemical potential μc = 0.2 eV, thickness of 0.1 nm, relaxation time τ = 1 ps, at temperature T = 293K. Graphene is incorporated into the antenna for its exceptional electrical conductivity, high electron mobility, tunable electrical properties and capability to support surface plasmon polaritons at THz frequencies, all of which significantly enhance the antenna's performance and efficiency in the THz range. Furthermore, the remarkable mechanical strength, flexibility, and lightweight properties of graphene contribute to the overall robustness and durability of the antenna, making it a highly effective material for this application. These characteristics collectively position graphene as an excellent material for THz antennas, providing notable advantages over the conventional materials typically used in GHz-range microstrip patch antennas. Additionally, the inherent simplicity and computational efficiency of the Transmission Line model make it an ideal choice for initial design exploration and optimization in THz antenna engineering. PBG structures are also commonly referred to as photonic crystals. Additionally, the design particulars of the THz antenna presented herein, which utilize two distinct types of PBG substrates, are also elaborated upon. To facilitate clarity throughout this document, the subsequent terminology will be employed to distinguish between the various antenna variants under discussion.

Ant I: The THz antenna, which is mounted on a consistent substrate, serves as a benchmark for assessing the effectiveness of alternative antennas, as depicted in Fig. 1a.

Ant II: The THz antenna is situated on a substrate designed with a PBG structure. The substrate comprised air cylinders. These air holes possess a lattice with a uniform radius of 15 μm, evenly spaced at 120 μm intervals, and match the substrate's thickness of 25 μm, as illustrated in Fig. 1b.

Ant III: The THz antenna is positioned on a PBG substrate, which incorporates circular and rectangular-shaped insertions. These insertions have dimensions defined by side length "Li" and width "Wi" and are separated from each other by 120 μm, as presented in Fig. 1c.

Ant IV: The THz antenna is supported by a Photonic Band Gap substrate and includes a graphene load introduced into the single patch, as pictured in Fig. 1d.

The rectangular patch's dimensions are selected to achieve resonance at the corresponding frequency. The patch's wp (width) and lp (length) are obtained utilizing the equations outlined in Refs. [34,35].

$$w_p = \frac{c}{2f_r}\sqrt{\frac{2}{1+\varepsilon_r}} \tag{1}$$

$$\varepsilon_{reff} = \frac{1+\varepsilon_r}{2} + \left(\frac{\varepsilon_r - 1}{2}\right)\left(1 + \frac{12h}{W}\right)^{-1/2} \tag{2}$$

Table 1
Dimensions of the THz antennas.

Component	Prameter	Value (um)
Ground	Length Lg	590
	Widh Wg	590
	Thickness hg	8
Substrat	Length Ls	590
	Widh Ws	590
	Thickness hs	25
	r	15
	d	60
	Lr	20
	Wr	30
Patch	Length Lp	255
	Widh Wp	250
	Thickness hp	8
Graphene	Wi	90
	Wj	65

$$l_p = \frac{c}{\sqrt{\varepsilon_{reff}} 2 f_r} - 2\Delta L \tag{3}$$

$$\Delta L = \frac{0.412h\left(\varepsilon_{reff} + 0.3\right)\left(\frac{w_p}{h} + 0.264\right)}{\left(\varepsilon_{reff} - 0.258\right)\left(\frac{w_p}{h} + 0.8\right)} \tag{4}$$

In these calculations, ε_r represents the relative permittivity, and h denotes the thickness of the polyimide substrate. The corporate feed technique is commonly employed for compact antenna designs due to its structural simplicity. In this technique, the feed line is engineered to have an input impedance of 50 Ω and to distribute power equally [36, 37]. The suggested antenna's dimensions are outlined in Table 1. The CST Microwave Studio Suite has been utilized to simulate and develop the suggested antenna.

Graphene, with its remarkable chemical properties, optical, and physical, has recently captured significant attention in the materials field, specifically in the domain of THz communications [38]. Its robust electrical conductivity fluctuates with alterations in frequency and other factors. Graphene can be represented as an ultra-thin conductive layer with surface conductivity (σs) consisting of two components: intraband (σintra) and interband (σinter) conductivity. These characteristics can be mathematically delineated through the use of Kubo's formula [39].

$$\sigma_{intra} = -\frac{e^2 k_B T}{\hbar^2 \pi}\left(\frac{\mu_c}{k_B T} + 2\ln\left(e^{-\frac{\mu_c}{k_B T}} + 1\right)\cdot\frac{j}{w - j\tau^{-1}}\right) \tag{5}$$

$$\sigma_{inter} = -\frac{je^2}{4\hbar^2 \pi}\ln\left(\frac{2|\mu_c| - (w - j\tau^{-1})\hbar}{2|\mu_c| + (w - j\tau^{-1})\hbar}\right) \tag{6}$$

$$\sigma_s = \sigma_{intra} + \sigma_{\text{inter}} \tag{7}$$

In the equations mentioned above, μc stands for the chemical potential of graphene, which can be altered by applying an electrostatic bias or bias voltage to the graphene [40]. Temperature is denoted as T. Furthermore, e symbolizes the elementary charge of an electron, ħ corresponds to the reduced Planck's constant, j represents the imaginary unit, k_B represents Boltzmann's constant, ω signifies the angular frequency, and τ is the relaxation time. However, within the THz frequency band, the energy of photons is significantly lower than the Fermi energy (EF ≫ kBT). As a result, the σintra component predominates, and the σinter component of graphene's conductivity becomes insignificant [40]. Consequently, the conductivity of graphene can be more succinctly represented by utilizing the Drude model [41].

$$\sigma(\omega, \mu_c, \tau) = \frac{e^2 \mu_c}{\hbar^2 \pi}\frac{j}{\omega + j\tau^{-1}} \tag{8}$$

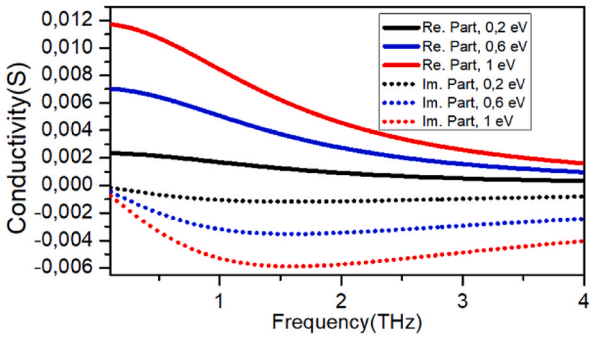

Fig. 2. Conductivity of graphene at various chemical potentials.

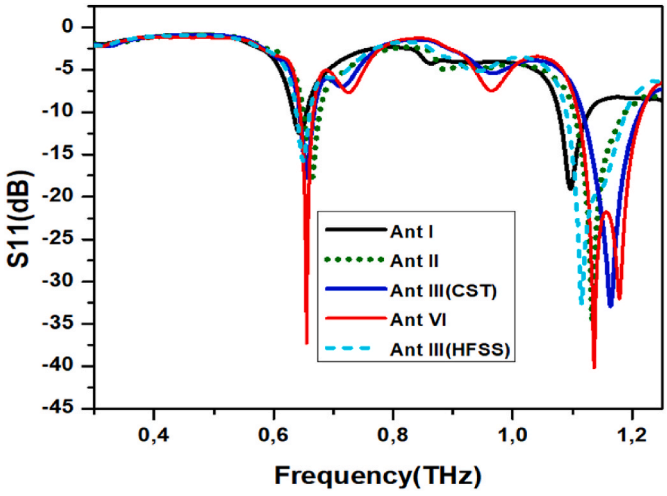

Fig. 3. Return loss characteristics of different antenna.

Reference [42] provides an approximate closed-form formula for calculating μc using the bias voltage Vg.

$$\mu_c \approx \hbar V_f \sqrt{\frac{\pi V_g \varepsilon_0 \varepsilon_r}{e t_s}} \tag{9}$$

In this context, ε_0 represents the vacuum permittivity, ε_r denotes the relative permittivity, v_f stands for the Fermi velocity in graphene (1.1×10^6 m/s), t_s represents the distance between the graphene layer and the electrode, and Vg signifies the applied bias voltage to the graphene. Fig. 2 displays the real and Imaginary components of graphene conductivity in terms of μc, which significantly influence the resonant frequency of the antenna. It's evident that as the frequency varies, the graphene conductivity also changes. The change in resonant amplitude is contingent on the real part of conductivity, while the shift in resonance range is determined by the conductivity's imaginary part. As depicted in Fig. 2, enhanced performance is achieved with a higher chemical potential, leading to an increase in graphene conductivity.

3. Results and analysis

The radiation properties of the recommended antennas have been assessed within the frequency band of 0.3–1.25 THz, employing the finite integration technique as made accessible in CST, as referenced in Ref. [43]. This analysis aimed to validate the precision of the recommended antenna design. Subsequently, the microstrip antenna's performance, designed with photonic crystals, was compared with a counterpart mounted on a homogeneous substrate. Various performance metrics, including return loss (S11), bandwidth (GHz), VSWR (Voltage Standing Wave Ratio), gain (dB), and radiation efficiency (%), were

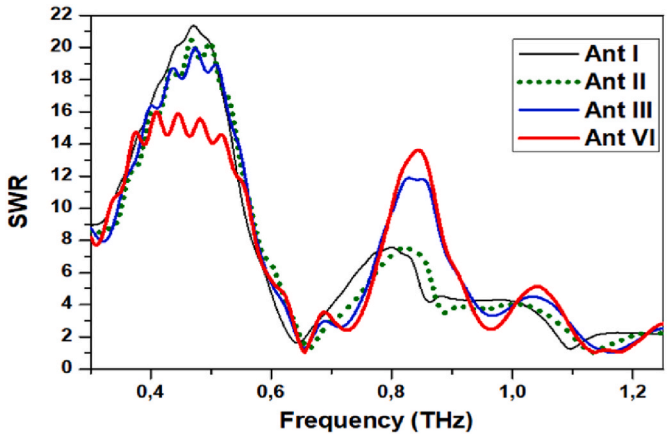

Fig. 4. SWR characteristic of the recommended antenna.

examined to understand the impact of photonic crystals on the performance of the antenna and to provide a comprehensive comparison between the two configurations.

According to Fig. 3, which depicts the value of the parameter S11 magnitudes for the various antenna designs. The operation spanning multiple bands across this frequency spectrum is observed. Antenna II demonstrates a notable deep reflection coefficient of −17.866 dB at 0.66 THz and −34.613 dB at 1.13 THz, resulting in a −10 dB bandwidth of 23.47 GHz and 80.8 GHz, respectively. Comparatively, Antenna III exhibits a reflection coefficient of −17.68 dB at 0.65 THz and −32.662 dB at 1.16 THz, indicating an improvement compared to Antenna I, which had S11 values of −12.557 dB and −19.014 dB, respectively. Notably, Antenna III, designed with an aperiodic Photonic Band Gap (PBG), resonates at 0.65 THz and 1.16 THz, with a bandwidth of 20.8 and 91.7 GHz, respectively. The Ant I (homogeneous substrate) exhibited peak resonance at 0.64 THz and 1.09 THz, with a bandwidth of 19.4 GHz and 50 GHz, respectively. In step four the suggested antenna (Ant VI) with load graphene has a return loss of −36.8 dB (BW = 25 GHz), and −41.812 dB (BW = 110 GHz) at 0.65 THz and 1.13 THz respectively. Moreover, the simulations conducted with CST and HFSS (High-Frequency Structure Simulator) for Ant III exhibit strong concordance, affirming the credibility of the recommended antenna design. The slight variation is attributable to the distinct calculation methods employed by each solver. This comparison demonstrates that when compared to the other antennas, especially Ant I, the aperiodic PBG with load graphene antenna gave greater bandwidth. The Ant I had poor performance, such as narrow bandwidth, because of the high surface waves in the uniform substrate, but after using the PBG substrate and graphene, the performance significantly improved. The unique feature of this study involves improving the performance of microstrip antennas through the utilization of a photonic crystal substrate with a load of graphene. Therefore, the increase in bandwidth can be credited to the integration of graphene and the adoption of an aperiodic PBG structure, which collectively elevates the electromagnetic characteristics of the antenna. Graphene's remarkable electrical conductivity, along with the PBG's capacity to suppress surface waves and enhance impedance matching, contributes to a wider operational bandwidth and deeper reflection coefficients.

Fig. 4 provides the VSWR for the recommended antennas, which encompass those utilizing PBG substrate, graphene load, and the uniform substrate, at their respective resonant frequencies, assessed through CST analysis. The VSWR, often viewed as the indicator of

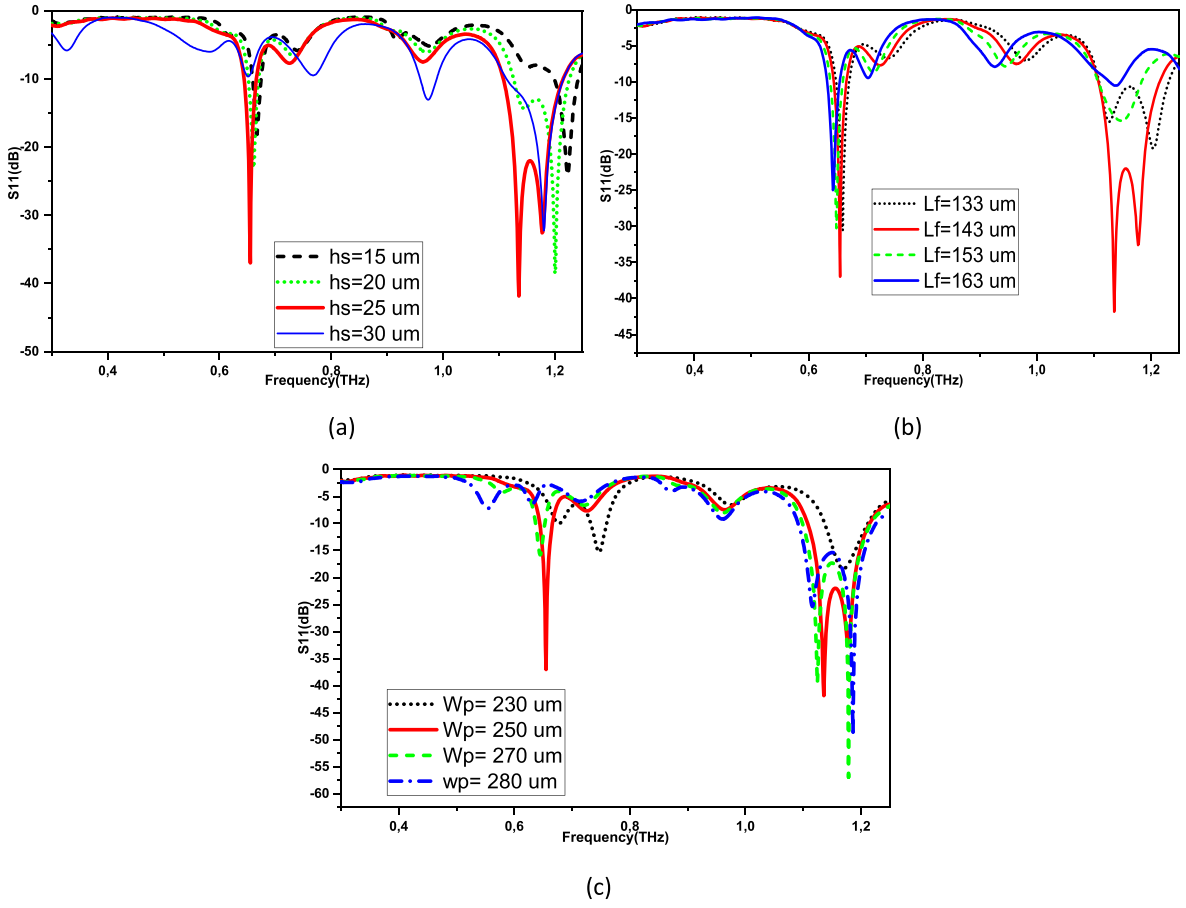

Fig. 5. Effect of tuning (a) hs, (b) Lf and (c) Wp on S11.

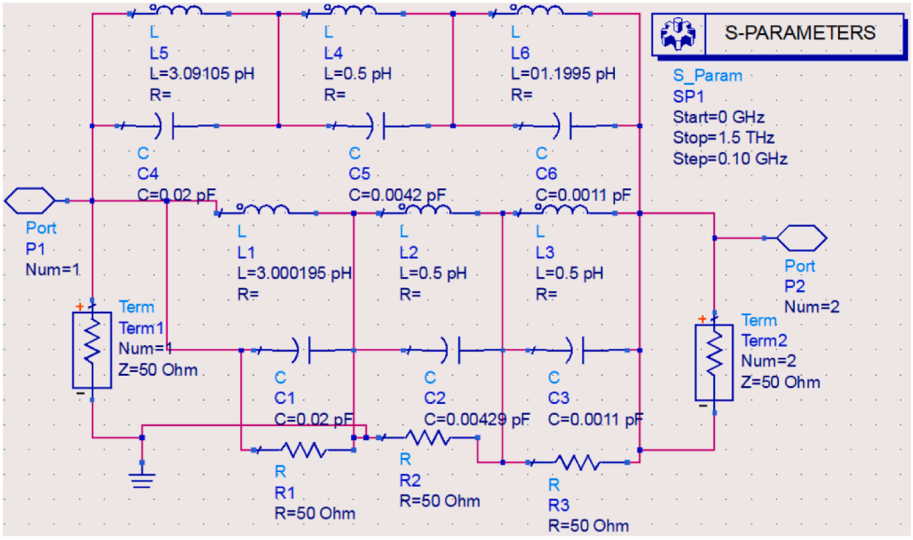

Fig. 6. Antenna's equivalent circuit.

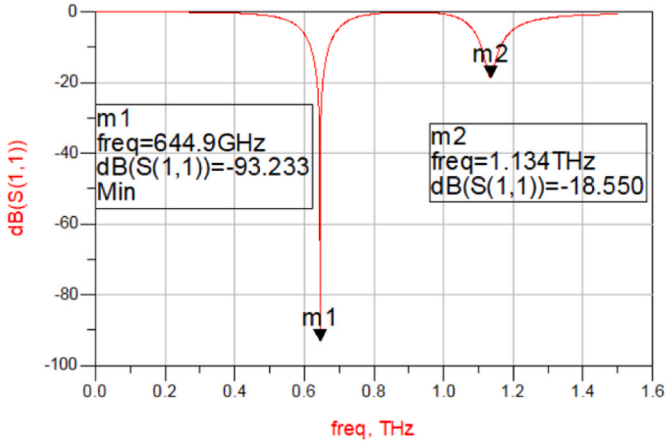

Fig. 7. Evaluating S11 for the proposed antenna via ADS.

antenna matching, typically falls within the range of 1–2 [44]. As illustrated in Fig. 4, the SWR for all four antennas was observed to be below 2 across the operational bandwidth, suggesting effective matching to the feed line. For the homogeneous substrate (Ant I), the SWR values are measured at 1.62 for the lower band frequency and 1.26 for the upper band frequency. In contrast, for the Antenna designed with periodic photonic crystals (Ant II), the SWR values are close to 1.3 for the lower band frequency and 1.04 for the second band frequency. These SWR values reflect the good matching between the antennas and the feed line, with Antenna II showing slightly better matching characteristics, particularly at the upper band frequency. In the third case (Ant III) the antenna has a SWR of 1.3, and 1.05 at the resonating frequency, and this value is close to 1.03, and 1.08 at the upper and lower band frequency respectively in the fourth step (Ant VI).

Fig. 5 illustrates the impact of the substrate thickness (hs), the feed line length (Lf), and the patch width (Wp) on the return loss of the recommended antenna. It is evident that the operating frequency bands are optimal at a substrate thickness of hs = 25 μm. As hs decreases, the S11 value decreases, resulting in a narrower bandwidth, as shown in

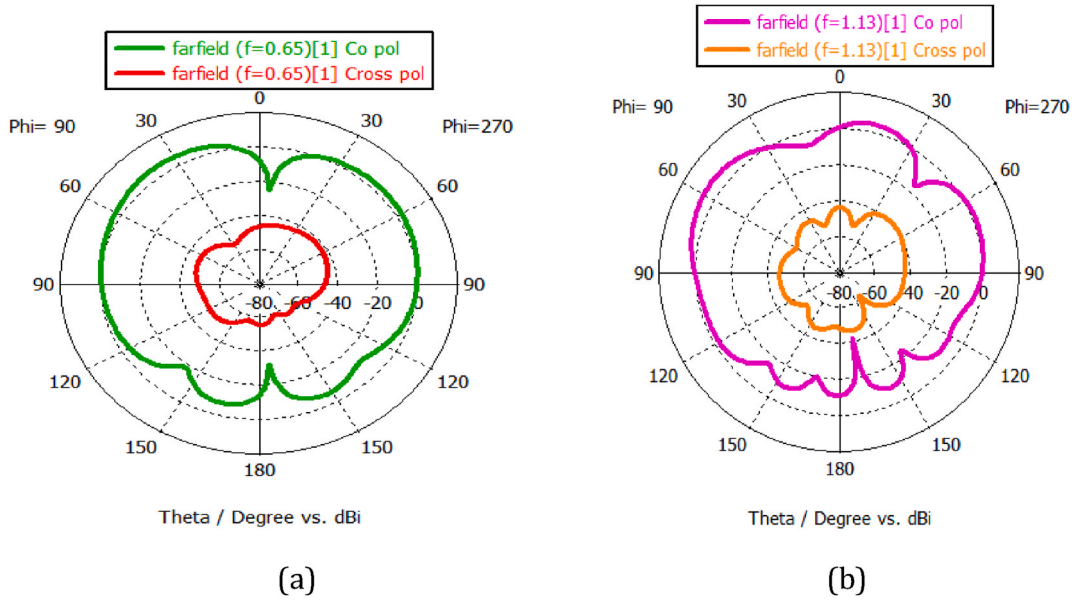

Fig. 8. co-polarized and cross polarized radiation patterns for the suggested antenna at (a) 0.65 THz and (b) 1.13 THz.

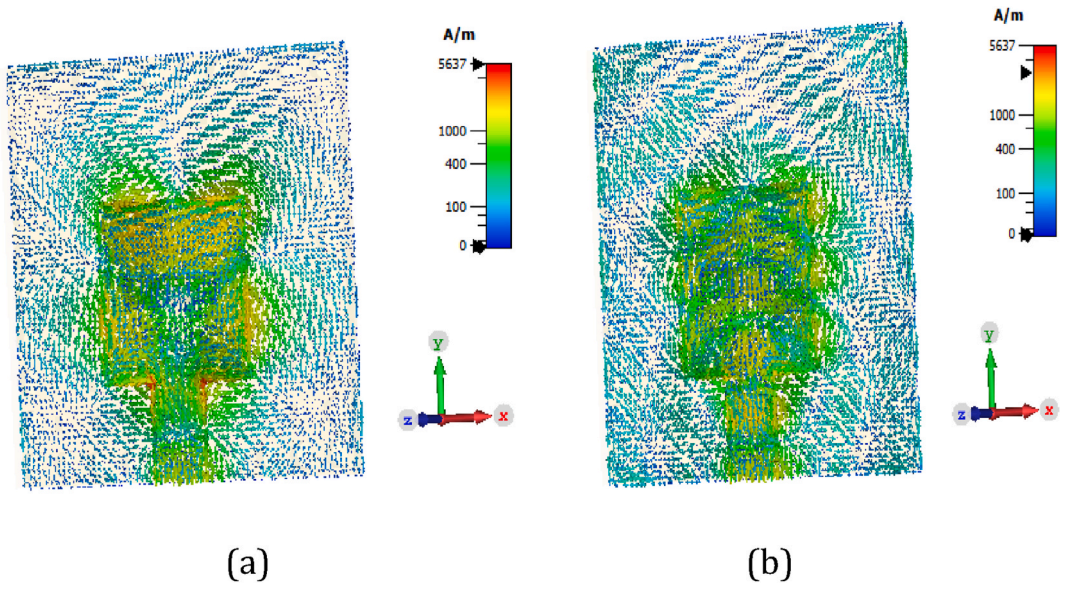

Fig. 9. Surface Current analysis of the antenna at (a) 650 THz, and (b) 1.13 THz.

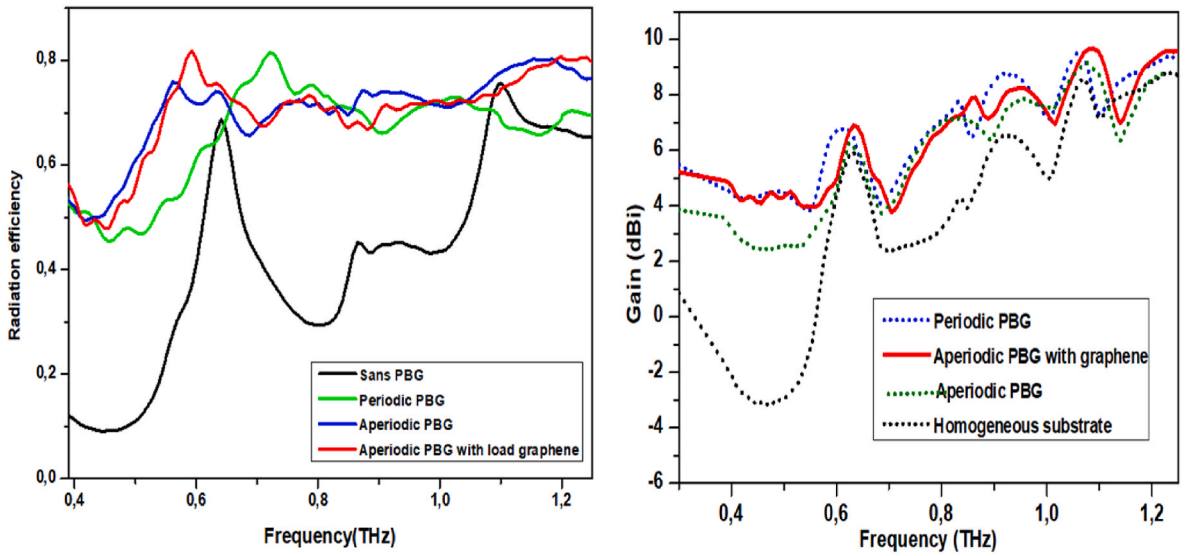

Fig. 10. (a) Radiation efficiency, and (b) Gain of the recommended dual-band antenna.

Fig. 5a. Additionally, the resonant frequencies shift to 0.97 THz and 1.18 THz when hs = 30 μm. As illustrated in Fig. 5b, the length of the feed line Lf significantly impacts S11. It increases from 133 to 163 μm. The optimized Lf is 143 μm, where the antenna achieves a maximum bandwidth of 25 GHz and 110 GHz with reflection coefficients of −37.3 dB and −41.812 dB at resonant frequencies of 0.65 THz and 1.13 THz, respectively. For all other Lf values, the antenna exhibits lower bandwidth and higher return loss. The impact of the patch width (Wp) on the S11 is depicted in Fig. 5c. The Wp varied from 230 μm to 280 μm, with Wp = **250** μm yielding the highest performance in terms of reflection coefficient and bandwidth, as illustrated in Fig. 5c. Consequently, the optimized dimensions for the proposed antenna are hs = 25 μm, Lf = 143 μm, and Wp = 250 μm.

The final approximated equivalent circuit model in ADS software, after adjusting the inductance (L), capacitance (C), and resistance (R) values, is presented in Fig. 6. The antenna's main feeder is represented by a parallel combination of L, C, and R [45]. Fig. 7 displays the S11 parameter for the recommended antenna using ADS. There is a strong correlation between the simulated results in CST and ADS (see Fig. 7).

Polarization can be classified into two main categories: cross-polarization and co-polarization [46]. Co-polarization occurs in the plane of radiation, aligning with the desired direction of the antenna. On the other hand, the undesirable radiations released from a linearly polarized antenna exhibit cross-polarization, with their orientation being perpendicular to the intended radiation direction. The simulated characteristics of co-polarization and cross-polarization for the THz antenna are presented in Fig. 8. The figure indicates that the levels of cross-polarization remain low for the antenna structures. The cross-polarization levels are measured at −42.9 dBi at 0.65 THz and −39.8 dBi at 1.13 THz, which are lower compared to the co-polarization levels, indicating a significant difference from the co-polarization levels. Fig. 9 presents the surface current of an antenna featuring a non-periodic Photonic Band Gap (PBG) structure at its resonance frequencies with a 120-degree phase shift, as simulated using CST Microwave Studio. The

Table 2
Comparing the properties of dual-band antennas with related designs.

	Frequency (THz)	S11 (dB)	BW (GHz)	Gain (dBi)	SWR	Efficiency (%)	Size(μm^2)
[28]	2.6	−27	145.4	2.8	1	87.3	30 × 20
	3.35	−22	140.5	6.03	≥1	53.47	
[29]	0.96	−13.05	310	3.8	1.3	–	950 × 950
[30]	0.703	−50.9	26.4	5.24	1.005	–	210 × 180
[48]	0.63	−44.71	36.23	7.94	–	–	–
[47]	0.6289	−20.745	34.92	6.59	1.2054	82.46	800 × 600
	0.6308	−44.71	36.23	7.94	1.0115	85.71	
[49]	0.750	−35	70	5.71	–	86.58	208.98 × 433.2
[20]	0.69	−64.16	–	6.793	1.015	–	208 × 180
[50]	0.67	−24	–	7.3	–	–	500 × 500
This work	0.65	−37.3	25	6.44	1.03	75.12	590 × 590
	1.13	−41.812	110	9.45	1.08	80.03	

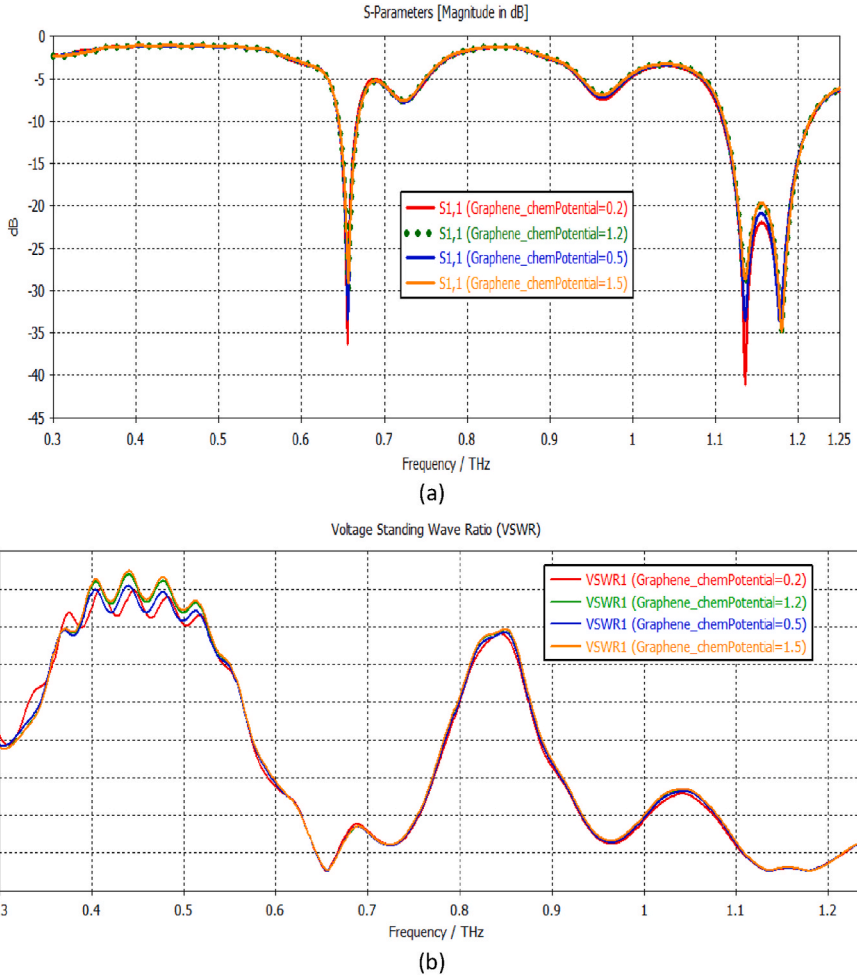

Fig. 11. (a) S11, and (b) SWR with the variation in μc.

design exhibits effective current dispersion across the entirety of the radiating element, as illustrated in Fig. 9. The figure clearly shows that the power transmitted from the feed line flows through the patch and radiates into the air, with most of the power being emitted from the substrate. Utilizing a non-periodic PBG substrate proves advantageous by maximizing radiated power and significantly reducing the reflected power at the antenna-air interface.

Additionally, for the sake of clarity, Fig. 10 demonstrates the enhancements obtained with the suggested antennas in the frequency band of 0.3–1.25 THz. It can be observed in Fig. 10 (b) that the aperiodic PBG with graphene antenna (Ant VI) gave a maximum gain of 9.45 dBi at the upper band frequency, as compared to the remaining three THz antennas. The radiation efficiency comparison depicted in Fig. 10 (a) reveals that the THz antennas based on PBG with load graphene exhibit higher efficiency, with values of 75.12 % and 80.03 % at the corresponding frequencies. This efficiency is notably superior to the other antennas, particularly Antenna I, which was implemented on a uniform substrate and achieved a radiation efficiency of 70 %. The improved efficiency of the PBG-based antennas can be attributed to the inhibition of surface waves facilitated by the PBG structure, allowing for more effective radiation and reduced losses. The manuscript evaluates the performance characteristics of THz antennas and contrasts them with antennas introduced in recent literature [20,28–30,47–50] in Table 2. The analysis demonstrates that the suggested antenna exhibits enhanced

outcomes concerning gain, S11, bandwidth, size and radiation efficiency. This antenna provides multi-band and high-gain THz operation suitable for various THz applications such as terahertz imaging systems and spectroscopic applications. Fig. 11 (a) and (b) illustrate how changes in μc affect the S11 and SWR of the recommended terahertz antenna PBG. The fluctuation in the chemical potential of the graphene material induces a change in the return loss while preserving the impedance bandwidth. The S11 of the recommended antenna shows significant improvement as μc decreases. For instance, when μc = 0.2 eV, the S11 of the antenna is −37.3 dB, −41.81 dB at resonant frequencies. These results demonstrate that varying the chemical potential μc effectively influences the return loss of the antenna, albeit with only minor modifications to the SWR.

4. Conclusion

In a comprehensive analysis covering a frequency span from 0.3 to 1.25 THz, a multiband antenna constructed with a photonic crystal is examined. This antenna showcases a remarkable maximum bandwidth of 110 GHz. During the assessment, it was determined that the antenna's minimum return loss is −41.812 dB, as obtained by CST Microwave Studio. The THz antenna presented in this study is subjected to a comparative analysis with other THz antennas that have been previously reported. The results demonstrate notable improvements in terms of both gain and bandwidth. Consequently, the amalgamation of PBG's unique properties and the antenna's multiband functionality renders it a highly promising solution for terahertz imaging systems, notably in security domains like airports, where detecting concealed items is crucial. Moreover, its applicability extends to biomedical imaging, presenting an opportunity to discern tissue irregularities with heightened precision and contrast. Despite the significant challenges inherent in constructing antennas with photonic crystal substrates and graphene layers, these obstacles can be effectively addressed through the application of advanced fabrication techniques, controlled environments, research into material compatibility, and scalable manufacturing processes. These strategies are poised to enable the realization of the full potential of our proposed antenna design. For our future endeavours, we can use the suggested antenna design and analysis methods to create a flexible multiband antenna. In future studies, we aim to design a PBG MIMO antenna array using the antenna introduced in this study.

Availability of data and materials

Data will be made available on request.

CRediT authorship contribution statement

Amraoui youssef: Writing – original draft, Software, Resources, Methodology, Conceptualization, Writing – review & editing. **Imane Halkhams:** Writing – review & editing, Visualization, Validation, Supervision, Conceptualization, Resources. **Rachid El Alami:** Validation, Software, Funding acquisition, Supervision, Visualization. **Mohammed Ouazzani Jamil:** Project administration, Data curation, Conceptualization, Supervision, Validation. **Hassan Qjidaa:** Investigation, Funding acquisition, Formal analysis, Supervision.

Declaration of competing interest

The authors declare that they have no known competing financial interests or personal relationships that could have appeared to influence the work reported in this paper.

Data availability

No data was used for the research described in the article.

References

[1] A. Bharadwaj, S. Vincent, T. Ali, The floret antenna for terahertz applications, Optik 272 (2023) 170335, https://doi.org/10.1016/j.ijleo.2022.170335.

[2] Y.H. Tao, A.J. Fitzgerald, V.P. Wallace, Non-contact, non-destructive testing in various industrial sectors with terahertz technology, Sensors 20 (3) (2020) 712.

[3] X. Zhang, T. Chang, Z. Wang, H.-L. Cui, Three-dimensional terahertz continuous wave imaging radar for nondestructive testing, IEEE Access 8 (2020) 144259–144276.

[4] O.P. Kumar, P. Kumar, T. Ali, P. Kumar, S. Vincent, Ultrawideband antennas: growth and evolution, Micromachines 13 (1) (2021) 60, https://doi.org/10.3390/mi13010060.

[5] H. Du, et al., Performance and optimization of reconfigurable intelligent surface aided THz communications, IEEE Trans. Commun. 70 (5) (2022) 3575–3593.

[6] S. Razavian, A. Babakhani, Silicon integrated THz comb radiator and receiver for broadband sensing and imaging applications, IEEE Trans. Microw. Theor. Tech. 69 (11) (2021) 4937–4950.

[7] A. Youssef, I. Halkhams, R. El Alami, M.O. Jamil, H. Qjidaa, Terahertz antennas: application, research challenges and future directions, in: The International Conference on Artificial Intelligence and Smart Environment, Springer, 2022, pp. 757–762, https://doi.org/10.1007/978-3-031-26254-8_109.

[8] T. Ramachandran, M.R.I. Faruque, K. Al-mugren, Low thermal SRR metamaterial design with multi-layered structured for terahertz frequency applications, Results in Engineering 21 (2024) 101753, https://doi.org/10.1016/j.rineng.2024.101753.

[9] P. Kumar, A.P. Dongare, T. Ali, S. Pathan, B.P. Shariff, O.P. Kumar, Characteristic mode analysis based flower shape high gain THz antenna for imaging and defense applications, in: 2023 International Telecommunications Conference (ITC-Egypt), IEEE, 2023, pp. 7–11, https://doi.org/10.1109/ITC-Egypt58155.2023.10206299.

[10] P. Das, G. Varshney, Analysis of tunable THz antennas integrated with polarization insensitive frequency selective surfaces, Opt. Quant. Electron. 53 (11) (2021) 645, https://doi.org/10.1007/s11082-021-03320-0.

[11] O.P. Kumar, P. Kumar, T. Ali, P. Kumar, S.B. K, A quadruple notch UWB antenna with decagonal radiator and Sierpinski square fractal slots, J. Sens. Actuator Netw. 12 (2) (2023) 24, https://doi.org/10.3390/jsan12020024.

[12] S.G. Johnson, J.D. Joannopoulos, Introduction to photonic crystals: Bloch's theorem, band diagrams, and gaps (but no defects), Photonic Crystal Tutorial 1 (2003) 16.

[13] M.N.E. Temmar, A. Hocini, D. Khedrouche, M. Zamani, Analysis and design of a terahertz microstrip antenna based on a synthesized photonic bandgap substrate using BPSO, J. Comput. Electron. 18 (2019) 231–240.

[14] A. Bendaoudi, M. Berka, M. Debab, Z. Mahdjoub, Effects of ground plane on a square graphene ribbon patch antenna designed on a high-permittivity substrate with PBG structures, Frequenz 77 (7–8) (2023) 385–394, https://doi.org/10.1515/freq-2022-0149.

[15] M.E. Benlakehal, A. Hocini, D. Khedrouche, M.N.E. Temmar, T.A. Denidni, Design and analysis of a 1× 2 microstrip patch antenna array based on periodic and aperiodic photonic crystals in terahertz, Opt. Quant. Electron. 54 (10) (2022) 672, https://doi.org/10.1007/s11082-022-03563-5.

[16] M.N.E. Temmar, A. Hocini, D. Khedrouche, T.A. Denidni, Analysis and design of MIMO indoor communication system using terahertz patch antenna based on photonic crystal with graphene, Photon. Nanostruct: Fundam. Appl. 43 (2021) 100867, https://doi.org/10.1016/j.photonics.2020.100867.

[17] F.M. de Sousa, F.B. de Sousa, I.R.S. Miranda, J.E. de Oliveira, W. Paschoal Jr., M.B. C. Costa, Graphene based nano patch antenna using photonic band gap insertion into substrate for applications at THz band, Opt. Quant. Electron. 55 (3) (2023) 210, https://doi.org/10.1007/s11082-022-04394-0.

[18] S.K. Danasegaran, E.C. Britto, S.C. Xavier, Exploration of trigonal patch antenna characteristics with the impact of 2D photonic crystal of various air hole shapes, J. Electron. Mater. 50 (9) (2021) 5365–5374, https://doi.org/10.1007/s11664-021-09071-8.

[19] R. Sachan, D.C. Dhubkarya, Photonic bandgap hepta-band stacked microstrip antenna for L, S and C band applications, Wireless Pers. Commun. 116 (3) (2021) 1913–1931, https://doi.org/10.1007/s11277-020-07771-8.

[20] S. Ullah, C. Ruan, T.U. Haq, X. Zhang, High performance THz patch antenna using photonic band gap and defected ground structure, J. Electromagn. Waves Appl. 33 (15) (2019) 1943–1954, https://doi.org/10.1080/09205071.2019.1654929.

[21] M.M. Fakharian, A graphene-based multi-functional terahertz antenna, Optik 251 (2022) 168431.

[22] D. Correas-Serrano, J.S. Gomez-Diaz, Graphene-based antennas for terahertz systems: a review, arXiv preprint arXiv:1704.00371 (2017), https://doi.org/10.48550/arXiv.1704.00371.

[23] A. Hocini, M. Temmar, D. Khedrouche, M. Zamani, Novel approach for the design and analysis of a terahertz microstrip patch antenna based on photonic crystals, Photon. Nanostruct: Fundam. Appl. 36 (2019) 100723.

[24] M.N. eddine Temmar, A. Hocini, D. Khedrouche, T.A. Denidni, Enhanced flexible terahertz microstrip antenna based on modified silicon-air photonic crystal, Optik 217 (2020) 164897.

[25] M.A.K. Khan, M.I. Ullah, M.A. Alim, High-gain and ultrawide-band graphene patch antenna with photonic crystal covering 96.48% of the terahertz band, Optik 227 (2021) 166056.

[26] Y. Dong, P. Liu, D. Yu, G. Li, F. Tao, Dual-band reconfigurable terahertz patch antenna with graphene-stack-based backing cavity, IEEE Antenn. Wireless Propag. Lett. 15 (2016) 1541–1544, https://doi.org/10.1109/LAWP.2016.2533018.

[27] T. Saeidi, I. Ismail, A.R. Alhawari, A. Sali, A. Ismail, High gain dual-band couple feed transparent THz antenna for satellite communications, in: 2016 IEEE Asia-Pacific Conference on Applied Electromagnetics (APACE), IEEE, 2016, pp. 11–15.

[28] J.N. George, M.G. Madhan, Analysis of single band and dual band graphene based patch antenna for terahertz region, Phys. E Low-dimens. Syst. Nanostruct. 94 (2017) 126–131, https://doi.org/10.1016/j.physe.2017.08.001.
[29] A. Singh, S. Singh, A trapezoidal microstrip patch antenna on photonic crystal substrate for high speed THz applications, Photon. Nanostruct: Fundam. Appl. 14 (2015) 52–62.
[30] L.C. Paul, M.M. Islam, Proposal of wide bandwidth and very miniaturized having dimension of μm range slotted patch THz microstrip antenna using PBG substrate and DGS, in: 2017 20th International Conference of Computer and Information Technology (ICCIT), IEEE, 2017, pp. 1–6, https://doi.org/10.1109/ICCITECHN.2017.8281766.
[31] K.V. Babu, G.N.J. Sree, T. Islam, S. Das, M.E. Ghzaoui, R.A. Saravanan, Performance analysis of a photonic crystals embedded wideband (1.41–3.0 THz) fractal MIMO antenna over SiO2 substrate for terahertz band applications, Silicon (2023) 1–14.
[32] M. Shalini, M.G. Madhan, Theoretical investigations on the influence of photonic crystal shapes on the performance of graphene-based terahertz photoconductive bowtie dipole antenna, Photon. Nanostruct: Fundam. Appl. 51 (2022) 101046.
[33] R.K. Kushwaha, P. Karuppanan, Enhanced radiation characteristics of graphene-based patch antenna array employing photonic crystals and dielectric grating for THz applications, Optik 200 (2020) 163422.
[34] L.C. Paul, M.H. Ali, N. Sarker, M.Z. Mahmud, R. Azim, M.T. Islam, A wideband rectangular microstrip patch antenna with partial ground plane for 5G applications, in: 2021 Joint 10th International Conference on Informatics, Electronics & Vision (ICIEV) and 2021 5th International Conference on Imaging, Vision & Pattern Recognition (icIVPR), IEEE, 2021, pp. 1–6, https://doi.org/10.1109/ICIEVicIVPR52578.2021.9564160.
[35] L.C. Paul, A.K. Sarkar, M.A. Haque, P. Miah, P.M. Ghosh, M.R. Islam, Investigation of the dependency of an inset feed rectangular patch antenna parameters with the variation of notch width for WiMax applications, in: 2018 Second International Conference on Electronics, Communication and Aerospace Technology (ICECA), IEEE, 2018, pp. 151–154, https://doi.org/10.1109/ICECA.2018.8474908.
[36] A. Youssef, I. Halkhams, R. El Alami, M.O. Jamil, H. Qjidaa, Study and design of a microstrip patch antenna array for 2.4 GHz applications, in: International Conference on Digital Technologies and Applications, Springer, 2023, pp. 309–317.
[37] A. Baz, D. Jansari, S.P. Lavadiya, S.K. Patel, Miniaturized and high gain circularly slotted 4× 4 MIMO antenna with diversity performance analysis for 5G/Wi-Fi/WLAN wireless communication applications, Results in Engineering 20 (2023) 101505, https://doi.org/10.1016/j.rineng.2023.101505.
[38] S. Fakhte, M.M. Taskhiri, Dual-band terahertz dielectric resonator antenna with graphene loading, Opt. Quant. Electron. 54 (12) (2022) 845, https://doi.org/10.1007/s11082-022-04229-y.
[39] G.W. Hanson, Dyadic Green's functions and guided surface waves for a surface conductivity model of graphene, J. Appl. Phys. 103 (6) (2008), https://doi.org/10.1063/1.2891452.
[40] M. Jafari Chashmi, P. Rezaei, N. Kiani, Polarization controlling of multi resonant graphene-based microstrip antenna, Plasmonics 15 (2020) 417–426, https://doi.org/10.1007/s11468-019-01044-2.
[41] S. Quader, J. Zhang, M.R. Akram, W. Zhu, Graphene-based high-efficiency broadband tunable linear-to-circular polarization converter for terahertz waves, IEEE J. Sel. Top. Quant. Electron. 26 (5) (2020) 1–8, https://doi.org/10.1109/JSTQE.2020.2969566.
[42] J. Gómez-Díaz, M. Esquius-Morote, J. Perruisseau-Carrier, Plane wave excitation-detection of non-resonant plasmons along finite-width graphene strips, Opt Express 21 (21) (2013) 24856–24872, https://doi.org/10.1364/OE.21.024856.
[43] A. Youssef, I. Halkhams, R. El Alami, M.O. Jamil, H. Qjidaa, A novel slotted antenna design for future Terahertz applications, Int. J. Electr. Comput. Eng. 14 (3) (2024) 2708–2716, https://doi.org/10.11591/ijece.v14i3.pp2708-2716.
[44] K.M.A. Kadhar, et al., Single input multiple output maze shaped array antenna for millimeter wave applications, Results in Engineering 22 (2024) 102097, https://doi.org/10.1016/j.rineng.2024.102097.
[45] L.C. Paul, et al., A low-profile antenna with parasitic elements and a DGS-based partial ground plane for 5G/WMAN applications, Discover Applied Sciences 6 (1) (2024) 22, https://doi.org/10.1007/s42452-024-05669-9.
[46] D.M. John, et al., A compact flexible four-element dual-band antenna using a unique defective ground decoupling structure for Sub-6 GHz wearable applications, Results in Engineering (2024) 101900, https://doi.org/10.1016/j.rineng.2024.101900.
[47] R.K. Kushwaha, P. Karuppanan, L. Malviya, Design and analysis of novel microstrip patch antenna on photonic crystal in THz, Phys. B Condens. Matter 545 (2018) 107–112.
[48] G. Bansal, A. Marwaha, A. Singh, Graphene based multiband frequency THz antennas for UWB applications, Int. J. New Innov. Eng. Technol. 12 (October 1) (2019).
[49] S. Anand, D.S. Kumar, R.J. Wu, M. Chavali, Graphene nanoribbon based terahertz antenna on polyimide substrate, Optik 125 (19) (2014) 5546–5549.
[50] A. Nejati, R.A. Sadeghzadeh, F. Geran, Effect of photonic crystal and frequency selective surface implementation on gain enhancement in the microstrip patch antenna at terahertz frequency, Phys. B Condens. Matter 449 (2014) 113–120, https://doi.org/10.1016/j.physb.2014.05.014.

View publication stats